Available online at www.sciencedirect.com

SciVerse ScienceDirect

Ceramics International 38 (2012) 1275–1279

CERAMICS INTERNATIONAL

www.elsevier.com/locate/ceramint

Ionic conductivity in $Bi_2Sn_2O_7$ ceramics

Rafael M. Almeida [a], Carlos William A. Paschoal [a,*], Jeffrey T. Auletta [b], Zachary R. Kann [b], Michael W. Lufaso [b]

[a] Departamento de Física - CCET, Universidade Federal do Maranhão, Campus do Bacanga, 65085-580 São Luís, MA, Brazil
[b] Department of Chemistry, University of North Florida, 1 UNF Drive, Jacksonville, FL 32224, USA

Received 30 May 2011; received in revised form 26 August 2011; accepted 27 August 2011
Available online 3 September 2011

Abstract

Impedance spectroscopy measurements, in the temperature range from room temperature to 600 K, were performed in order to investigate the dielectric and ionic properties of $Bi_2Sn_2O_7$ ceramics. The results show that the conductivity in this pyrochlore is associated with the hopping of ions. An activation energy of 1.26 eV was observed and the dielectric constant exhibits a strong contribution from ionic conduction.

Keywords: A. Powders: solid state reaction; B. Spectroscopy; C. Dielectric properties; C. Impedance; C. Ionic conductivity

1. Introduction

The $Bi_2Sn_2O_7$ (BSO) pyrochlore has attracted much attention in recent years due to various physical and chemical properties, notably including its catalytic properties, such as processes involving the oxidation of hydrocarbons [1] and isobutene [2–4] and its utilization in gas sensing materials [5–8]. $Bi_2Sn_2O_7$ was first prepared by Roth [9] and later, Brisse and Knop [10] showed that the room temperature crystal structure of this compound was closely related to, but distorted from, the ideal cubic pyrochlore structure. Vetter et al. [11] reported two different phases, an ideal cubic pyrochlore at high temperatures and a tetragonal phase at low temperatures. Shannon et al. [12] studied high purity crystals and observed three distinct phases. At temperatures above 680 °C they proposed that an ideal cubic pyrochlore structure, designated as the γ phase, is present. At intermediate temperatures, higher than 90 °C, a cubic acentric phase, designated as the β phase, is present according to the optical measurements. X-ray diffraction (XRD), electrical resistivity, and differential scanning calorimetry (DSC) measurements in polycrystalline BSO, performed by the same authors, suggest that the α → β phase transition happens near 135 °C. At room temperature, they observed that the structure is probably tetragonal and designated it as the α phase.

Shannon et al. also showed that the BSO exhibits second harmonic generation and domains at room temperature [12]. These domains disappear in the α → β phase transition near 90 °C, therefore this phase transition is possibly ferroic. The high electron density of Bi^{3+} and Sn^{4+} compared to that of the oxygen ions results in a lack of sensitivity using X-ray diffraction measurements, therefore neutron diffraction measurements were performed in order to examine the structure of γ phase [13,14]. Both investigations confirmed the structure of γ phase as the ideal cubic pyrochlore belonging to the $Fd\bar{3}m$ space group. The structure can be viewed as consisting of two interpenetrating networks: Bi_2O' chains and corner-sharing SnO_6, where the Bi^{3+} cation is eight-coordinated with scalenohedral geometry and the Sn^{4+} cation is six-coordinated in a trigonal antiprism [15]. The crystal structure of polycrystalline α-BSO was determined by Evans et al. [16] using Rietveld refinement of combined X-ray and neutron diffraction data. They showed that, from room temperature to 137 °C, BSO crystallizes in a very complicated monoclinic structure with 176 crystallographically independent atoms, which makes it one of the most complex oxide structures ever solved using powder diffraction techniques.

In spite of the high applicability of pyrochlore compounds as solid electrolytes in fuel cells [17,18], dielectrics in capacitors and microwave devices [19–23], to the best of our knowledge there are no reports about the ionic and dielectric properties of

* Corresponding author. Tel.: +55 98 3301 8291; fax: +55 98 3301 8204.
E-mail addresses: paschoal@ufma.br, paschoal@pq.cnpq.br (C.W.A. Paschoal).

0272-8842/$36.00
doi:10.1016/j.ceramint.2011.08.060

$Bi_2Sn_2O_7$. Thus, in this work, we present the high temperature dielectric and ionic properties of BSO ceramics investigated by impedance spectroscopy measurements.

2. Experimental procedures

Samples were synthesized by the solid state method from stoichiometric amounts of 99.975% Bi_2O_3 and 99.9% SnO_2 (cation basis, Alfa Aesar Chemical Company, USA). Prior to each heating cycle the sample was ground with an agate mortar and pestle under acetone for 10–15 min. Samples were heated in high form alumina crucibles. Specimens were initially heated at 750 °C for 12–24 h, then ground and reheated 3 times. Phase purity was ascertained, after each heating cycle, from X-ray powder diffraction data collected at ambient temperature using Cu *Ka* radiation and a Rigaku Ultima III diffractometer equipped with a graphite monochromator and a scintillation detector. Equilibrium was assumed when no further changes were evident in the relative intensities of the peaks. The Jade software package (Materials Data, Inc., Livermore, CA) was used in the phase analysis and Crystal Impact Diamond ver. 3.2 g was used to perform the XRD simulation.

The impedance spectroscopy measurements were performed by connecting a pellet of the sample in the form of a parallel plate capacitor to a Solartron Frequency Response Analyzer model 1260 coupled to a Solartron Dielectric Interface model 1296. The measurements were carried out in the frequency range from 1 Hz up to 1 MHz and in the temperature range from room temperature up to 600 K. The capacitor electrodes were deposited using silver paste. The temperature measurements were performed in a controlled EDG 10P furnace. All the measurements were performed under air.

3. Results and discussions

The X-ray diffraction pattern of $Bi_2Sn_2O_7$ is presented in Fig. 1. The inset of Fig. 1 shows the simulated X-ray pattern using the structure of Evans et al. [16]. In other studies of the Bi_2O_3–SnO_2 join, few other phases have been reported, but include a sillenite-related phase, $Bi_{12}SnO_{20}$ and a $Bi_{64}SnO_{98}$ phase grown from an oxide melt [24,25]. It was suggested $Bi_{12}SnO_{20}$ could only be prepared by quenching and was apparently unstable. The $Bi_2Sn_2O_7$ phase formed without any indication for unreacted starting materials, i.e., Bi_2O_3 or SnO_2, and there were no indications for other secondary phases in the X-ray diffraction pattern.

In Fig. 2 the complex plane of impedance for the BSO sample at several measured temperatures is shown. The impedance arc is distorted, indicating both grain and grain-boundary contributions. This behavior is more prominent at high temperatures, where the grain boundary contribution

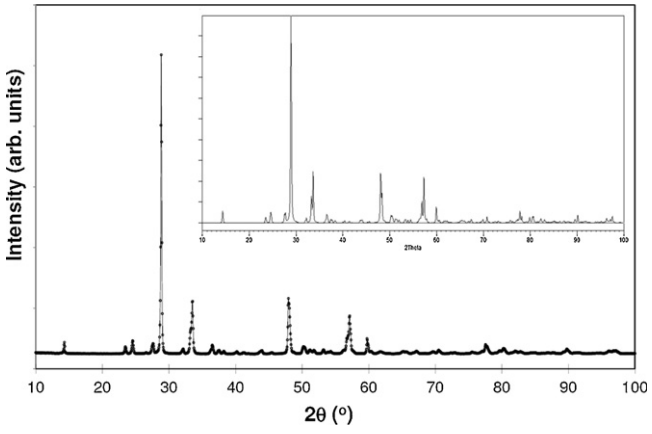

Fig. 1. Ambient temperature X-ray powder diffraction pattern of $Bi_2Sn_2O_7$. The inset shows the simulated X-ray diffraction pattern based on the 176 atom crystal structure, in space group Pc, as reported by Evans et al. [16].

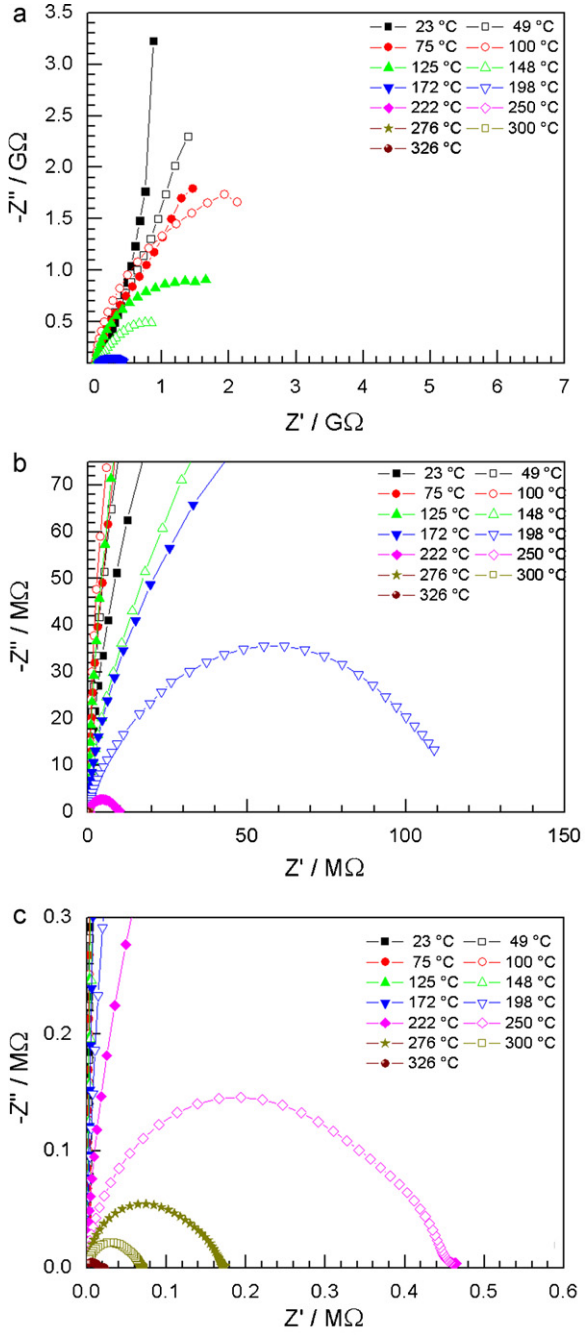

Fig. 2. Impedance complex plane (ICP) obtained for the $Bi_2Sn_2O_7$ sample. From (a) to (c) the ICP is enlarged to show all the graphs.

decreases showing that the grain contribution is bigger in this range [26,27]. These two contributions are better observed in the Bode graph of the imaginary part of the impedance, shown in Fig. 3. The presence of a distorted peak is clearly evident and this distortion is more pronounced at higher temperatures.

From the complex impedance we obtained the dielectric function. The temperature dependence of the real part of the dielectric constant is shown in Fig. 4. The real part of the dielectric constant (ε') increases with temperature, indicating a high ionic conductivity contribution to the dielectric constant. Moreover, we see that the dielectric constant does not show indubitable evidence of the structural phase transition near 125 °C, whose temperature is indicated by an arrow in Fig. 4.

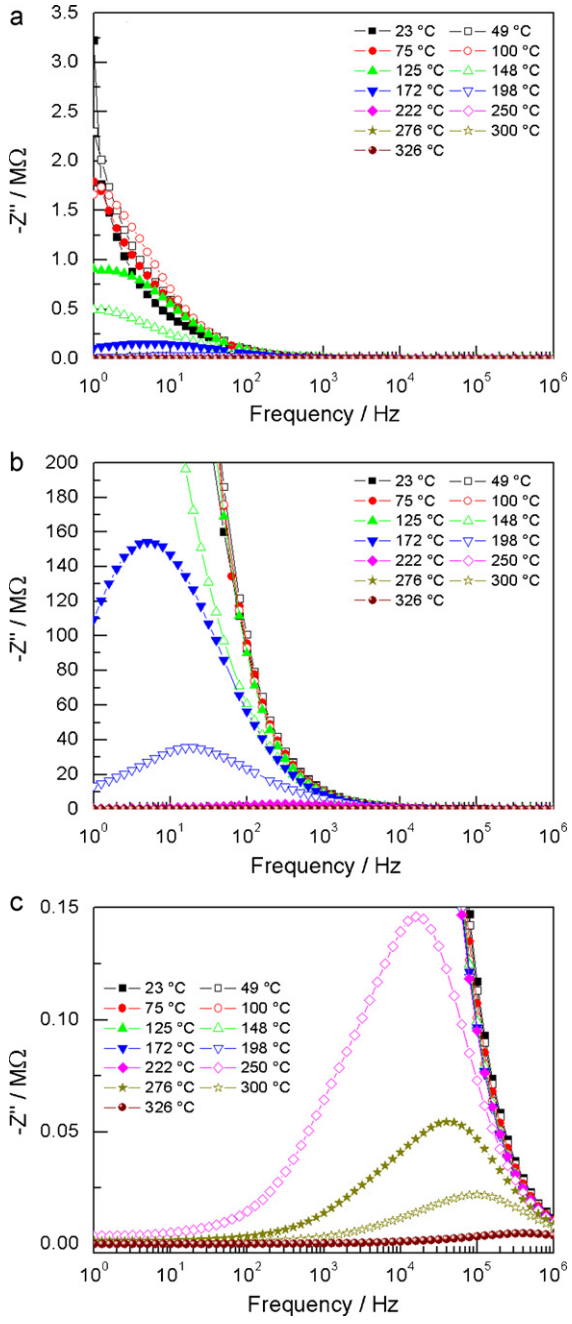

Fig. 3. Bode graph of the imaginary part of the impedance (Z'') obtained for the $Bi_2Sn_2O_7$ sample. From (a) to (c) the graph is enlarged to show the Z'' maxima.

Only a subtle step takes place in dielectric constant near this temperature.

The conductivity of BSO at several temperatures, presented in Fig. 5a, was obtained using the Maxwell relation $\sigma(\omega) = j\omega\varepsilon_o\varepsilon(\omega)$, where j is the pure imaginary, ε_o is the vacuum permittivity and $\varepsilon(\omega)$ is the dielectric constant of the sample obtained from the impedance response through the relation $\varepsilon(\omega) = [j\omega C_o Z(\omega)]^{-1}$, where C_o is the capacitance of the open cell. It is observed that, from low to high frequencies, σ' increases three orders of magnitude for temperatures equal or below 222 °C. However, for temperatures above that it does not change very much, indicating that the DC conductivity of the sample increases substantially at high temperatures. This information can be quantified by modeling the behavior of the conductivity using the equation [26,27]

$$\sigma = \sigma_0 + A\omega^{s(T)} + B\omega^{t(T)} \quad (1)$$

where A and B are temperature dependent constants, $s(T)$ and $t(T)$ are temperature and frequency dependent parameters close to unity, and σ_0 is correlated with the DC conductivity. We observe that for high temperatures the conductivity is practically constant in the frequency range investigated and does not exhibit dispersion. The temperature dependence of conductivity parameters clearly shows the structural phase transition and it is evident that B e $t(T)$ are parameters related to the grain boundary once their temperature dependence is weak compared to the same dependence of A and $s(T)$ parameters, as shown in Fig. 5b and c.

The reciprocal temperature dependence of the conductivity is shown in Fig. 6. The conductivity exhibits standard dielectric behavior, i.e., it shows a baseline for different frequencies and it tends toward the same value at higher temperatures. Furthermore, the conductivity follows the Arrhenius behavior given by the equation

$$\sigma = \sigma_0 \exp\left(\frac{-E_a}{kT}\right) \quad (2)$$

where E_a is the activation energy and k is the Boltzmann constant. From this it is also possible to estimate the activation

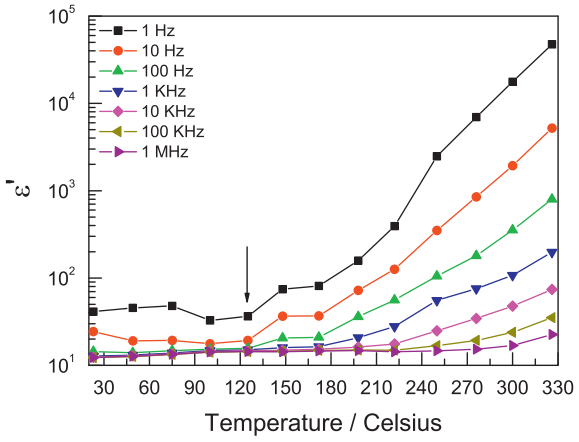

Fig. 4. Temperature dependence of the real part of permittivity (ε') obtained for the $Bi_2Sn_2O_7$ sample. The arrow indicates the temperature of the structural phase transition.

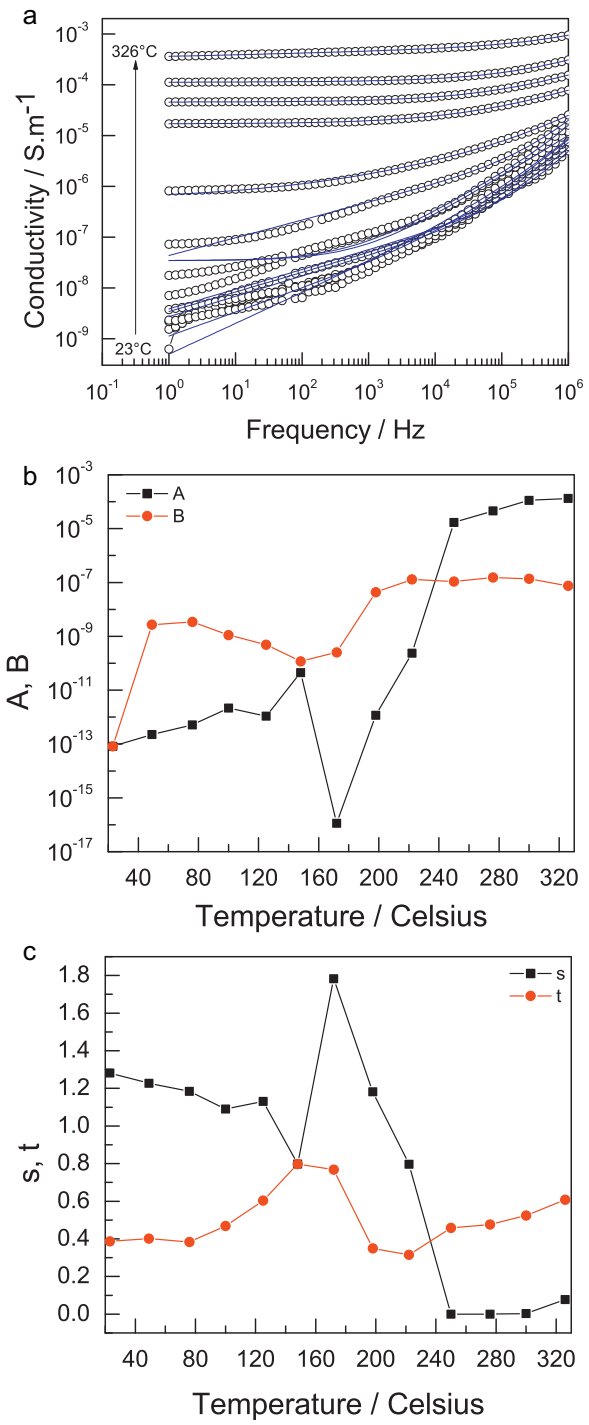

Fig. 5. Frequency dependence of the real part of the conductivity at several temperatures. (b and c) The dependence with temperature of the conductivity parameters according to the model given by Eq. (1).

energy. The activation energy obtained at 1 kHz is 1.26 eV and has a magnitude on the order of the oxygen vacancy motion, as observed for Ba_2BiSbO_6 (1.14 eV) [26] and $SrFe_{1/2}Nb_{1/2}O_3$ (1.26 eV) [28]. This energy value suggests that the conduction mechanism is associated with the hopping of ions between neighboring sites within the crystal lattice.

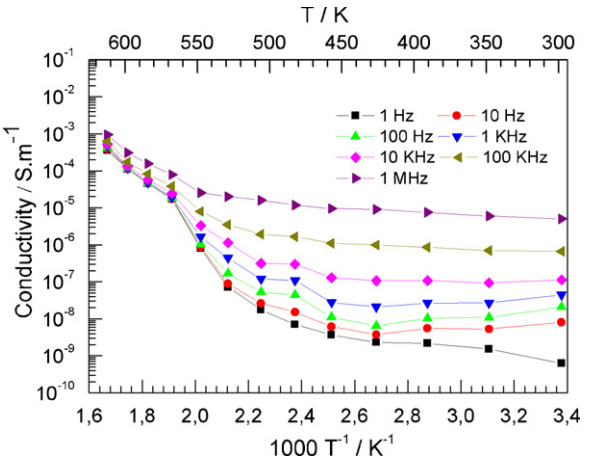

Fig. 6. Temperature dependence of conductivity obtained for the $Bi_2Sn_2O_7$ sample. The lines are the guide to the eyes.

4. Conclusions

Impedance spectroscopy measurements in bismuth stannate ($Bi_2Sn_2O_7$) were performed in the temperature range from room temperature to 600 K. The conduction mechanism at temperatures higher than T_c has an activation energy on the order of 1.26 eV and suggests that the conduction mechanism is associated with the hopping of ions between neighboring sites within the crystal lattice. Additionally, the temperature dependence of the dielectric constant exhibits only subtly the $\alpha \rightarrow \beta$ structural phase transition.

Acknowledgements

The Brazilian authors acknowledge the financial support from CNPq, CAPES and FAPEMA Brazilian funding agencies. MWL acknowledges financial support from Research Corporation and UNF for the Munoz Professorship.

References

[1] C.A. Mims, A.J. Jacobson, R.B. Hall, J.T. Lewandowski, Methane oxidative coupling over nonstoichiometric bismuth-tin pyrochlore catalysts, J. Catal. 153 (1995) 197–207.
[2] L. Moens, P. Ruiz, B. Delmon, M. Devillers, Cooperation effects towards partial oxidation of isobutene in multiphasic catalysts based on bismuth pyrostannate, Appl. Catal. A-Gen. 171 (1998) 131–143.
[3] L. Moens, P. Ruiz, B. Delmon, M. Devillers, Evaluation of the role played by bismuth molybdates in $Bi_2Sn_2O_7$–MoO_3 catalysts used for partial oxidation of isobutene to methacrolein, Appl. Catal. A-Gen. 180 (1999) 299–315.
[4] L. Moens, P. Ruiz, B. Delmon, M. Devillers, A simplified partial ionic charge model to evaluate the role played by bismuth pyrostannate in multiphase catalysts for the selective oxidation of isobutene to methacrolein, Appl. Catal. A-Gen. 249 (2003) 365–374.
[5] G.S.V. Coles, S.E. Bond, G. Williams, Metal stannates and their role as potential gas-sensing elements, J. Mater. Chem. 4 (2004) 23–27.
[6] G. Sarala Devi, S.V. Manorama, V.J. Rao, SnO_2/Bi_2O_3: a suitable system for selective carbon monoxide detection, J. Electrochem. Soc. 145 (1998) 1039–1044.

[7] G. Sarala Devi, S.V. Manorama, V.J. Rao, SnO_2:Bi_2O_3 based CO sensor: laser-Raman, temperature programmed desorption and X-ray photoelectron spectroscopic studies, Sens. Actuators B 56 (1999) 98–105.
[8] T.D. Malinovskaya, A.I. Aparnev, Y.P. Egorov, Y.M. Yukhin, Carbon monoxide semiconductor sensors based on SnO_2–Bi_2O_3, Russ. J. Appl. Chem. 74 (2001) 1864–1867.
[9] R.S. Roth, Pyrochlore-type compounds containing double oxides of trivalent and tetravalent ions, J. Res. Nat. Bur. Stand. 56 (1956) 17–25.
[10] F. Brisse, O. Knop, Pyrochlores. 3. X-ray neutron infrared and dielectric studies of $A_2Sn_2O_7$ stannates, Can. J. Chem. 46 (1968) 859.
[11] G. Vetter, F. Queyroux, J.C. Gilles, Preparation, stability and preliminary crystallographic study on $Bi_2Sn_2O_7$ compound, Mater. Res. Bull. 13 (1978) 211–216.
[12] R.D. Shannon, J.D. Bierlein, J.L. Gillson, G.A. Jones, A.W. Sleight, Polymorphism in $Bi_2Sn_2O_7$, J. Phys. Chem. Solids 41 (1980) 117–122.
[13] V. Kahlenberg, T. Zeiske, Structure of gamma-$Bi_2Sn_2O_7$ by high temperature powder neutron diffraction, Z. Kristallogr. 212 (1997) 297–301.
[14] R.H. Jones, K.S. Knight, The structure of gamma-$Bi_2Sn_2O_7$ at 725 degrees C by high-resolution neutron diffraction: implications for bismuth(III)-containing pyrochlores, J. Chem. Soc. Dalton (1997) 2551–2555.
[15] M.A. Subramanian, G. Aravamudan, G.V.S. Rao, Oxide pyrochlores—a review, Prog. Solid State Chem. 15 (1983) 55–143.
[16] I.R. Evans, J.A.K. Howard, J.S.O. Evans, alpha-$Bi_2Sn_2O_7$—a 176 atom crystal structure from powder diffraction data, J. Mater. Chem. 13 (2003) 2098–2103.
[17] B.J. Wuensch, K.W. Eberman, C. Heremans, E.M. Ku, P. Onnerud, E.M.E. Yeo, S.M. Haile, J.K. Stalick, J.D. Jorgensen, Connection between oxygen-ion conductivity of pyrochlore fuel-cell materials and structural change with composition and temperature, Solid State Ionics 129 (2000) 111–133.
[18] J.A. Diaz-Guillen, M.R. Diaz-Guillen, K.P. Padmasree, A.F. Fuentes, J. Santamaria, C. Leon, High ionic conductivity in the pyrochlore-type $Gd_{2-y}La_yZr_2O_7$ solid solution ($0 <= y <= 1$), Solid State Ionics 179 (2008) 2160–2164.
[19] J.H. Park, C.J. Xian, N.J. Seong, S.G. Yoon, Bismuth-based pyrochlore thin films deposited at low temperatures for embedded capacitor applications, Jpn. J. Appl. Phys. 1 (45) (2006) 7325–7328.
[20] J. Park, J.W. Lu, S. Stemmer, R.A. York, Microwave dielectric properties of tunable capacitors employing bismuth zinc niobate thin films, J. Appl. Phys. 97 (2005) 084110.
[21] P.P. Rao, D.N. Rajendran, K.R. Nair, P. Koshy, V.K. Vaidyan, Microwave dielectric properties of new pyrochlore type oxides: $Pb_3R_3Ti_7Nb_2O_{26.5}$ (R = Y, Pr, Nd, Gd or Dy), Mater. Sci. Eng. B-Solid 128 (2006) 184–187.
[22] Y.C. Lee, Y.P. Hong, D.M. Kim, K.H. Ko, Very high tunable inter-digital capacitor using bismuth zinc niobate thin-film dielectrics for microwave applications, Electron. Lett. 42 (2006) 851–853.
[23] M.M.A. Sekar, K.C. Patil, Low-temperature synthesis and properties of microwave resonator materials, Mater. Sci. Eng. B-Solid 38 (1996) 273–279.
[24] G. Huo, J. Lu, L. Ren, Phase relations in the Bi_2O_3–CoO_y–SnO_2 system at room temperature, J. Alloys Compd. 368 (2004) 126–129.
[25] Gattow, Fricke, Bismuth oxides. IV. The binary systems of Bi2O3 with SiO2, GeO2, and SnO2, Zeitschrift fuer Anorganische und Allgemeine Chemie 324 (5/6) (1963) 287–296.
[26] M.C. Castro Jr., C.W.A. Paschoal, F.C. Snyder, M.W. Lufaso, Relaxations in Ba_2BiSbO_6 double complex perovskite ceramics, J. Appl. Phys. 104 (2008) 104114.
[27] A. Huanosta-Tera, R. Lira-Hueso, O. Perez-Orta, S.A. Palomares-Sanchez, S. Ponce-Castaneda, M. Mirabal-Garcia, Electric characterization of (Sr, Sr–Ba, Ba) M-type ferrites by ac measurements, Scr. Mater. 42 (2000) 603–607.
[28] Y.Y. Liu, X.M. Chen, X.Q. Liu, L. Li, Giant dielectric response and relaxor behaviors induced by charge and defect ordering in $Sr(Fe_{1/2}Nb_{1/2})O_3$ ceramics, Appl. Phys. Lett. 90 (2007) 192905.